

# Nuclear Magnetic Resonance studies of DNP-ready trehalose obtained by solid state mechanochemical amorphization

M. Filibian<sup>1</sup>, E. Elisei<sup>2,3</sup>, S. Colombo Serra<sup>4</sup>, A. Rosso<sup>5</sup>, F. Tedoldi<sup>4</sup>, A. Cesàro<sup>2,6</sup> and P. Carretta<sup>1</sup>

<sup>1</sup> *University of Pavia, Department of Physics, Via Bassi 6, 27100-Pavia, Italy*

<sup>2</sup> *Department of Chemical and Pharmaceutical Sciences,*

*University of Trieste, Via Giorgieri 1, 34127 Trieste, Italy*

<sup>3</sup> *UMET, Unité Matériaux et Transformations, CNRS, Univ. Lille, F-59000 Lille, France*

<sup>4</sup> *Centro Ricerche Bracco, Bracco Imaging Spa, via Ribes 5, 10010 Collettero Giacosa (TO), Italy.*

<sup>5</sup> *Laboratoire de Physique Théorique et Modèles Statistiques (UMR CNRS 8626),*

*Université Paris-Sud, Bât. 100, 15 rue Georges Clémenceau, 91405 Orsay Cedex, France*

<sup>6</sup> *Elettra Sincrotrone Trieste, Area Science Park, I-34149 Trieste, Italy.*

<sup>1</sup>H nuclear spin-lattice relaxation and Dynamic Nuclear Polarization (DNP) have been studied in amorphous samples of trehalose sugar doped with TEMPO radicals by means of mechanical milling, in the 1.6 K ÷ 4.2 K temperature range. The radical concentration was varied between 0.34 and 0.81 %. The highest polarization of 15 % at 1.6 K, observed in the sample with concentration 0.50%, is of the same order of magnitude of that reported in standard frozen solutions with TEMPO. The temperature and concentration dependence of the spin-lattice relaxation rate  $1/T_1$ , dominated by the coupling with the electron spins, were found to follow power laws with an exponent close to 3 in all samples. The observed proportionality between  $1/T_1$  and the polarization rate  $1/T_{\text{pol}}$ , with a coefficient related to the electron polarization, is consistent with the presence of Thermal Mixing (TM) and a good contact between the nuclear and the electron spins. At high electron concentration additional relaxation channels causing a decrease in the nuclear polarization must be considered. These results provide further support for a more extensive use of amorphous DNP-ready samples, obtained by means of comilling, in dissolution DNP experiments and possibly for *in vivo* metabolic imaging.

## I. INTRODUCTION

In the last decades Dynamic Nuclear Polarization (DNP) has become one of the most efficient and celebrated hyperpolarization techniques able to enhance the Nuclear Magnetic Resonance (NMR) signal by up to four orders of magnitude [1]. In particular DNP has been crucial for the development of *in vivo* real-time metabolic Magnetic Resonance Imaging (MRI) [2], high resolution NMR of biological samples [3, 4] and kinetic studies of nanostructured materials [5], where the detection of nuclei with low sensitivity in standard experimental conditions is unfeasible. For *in vivo* biomedical studies, before the dissolution and injection in the body, DNP is obtained at temperatures of the order of 1 K and in magnetic fields of few Tesla in samples prepared with special procedures [6, 7]. The hyperpolarization implies a microwave assisted transfer of polarization from unpaired electrons to the nuclei of a molecular substrate to be used *in vivo*. Thus, the DNP sample must contain a suitable amount of polarizing agents, typically radical compounds, which shall be intimately and homogeneously admixed to the molecular substrate of interest.

The sample preparation method significantly affects the DNP properties, namely its efficiency, and thus represents a major issue in the optimization and standardization of the hyperpolarization and dissolution process. In a few cases samples can be prepared directly by dissolving appropriate radicals in the pure substrate if this latter is liquid at room temperature, as pyruvic acid[8]. Alter-

natively, when the substrate is in solid form, a proper admixture with the polarizing agent is achieved either by dissolving the sample in a suitable solvent [3, 6, 7] or by melting the sample [3, 9]. In order to preserve a homogeneous spatial distribution of the radicals at low temperature, essential for an efficient DNP process, the liquid solution is typically cooled down rapidly to cryogenic temperatures so that a frozen amorphous state is achieved. In fact, an effective polarization cannot be reached in crystalline solids since upon crystallite formation the radicals are segregated to the surface and pushed far apart from the nuclei to be polarized[7].

The study of amorphization methods has been particularly relevant for DNP based metabolic MRI since many samples of diagnostic interest are crystalline solids at room temperature. Remarkably, a new method for the preparation of solvent-free amorphous mixtures of a crystalline solid substrate with radicals, ready for DNP, has been recently presented [10]. The method is based on mechanical milling, which is extensively used in the pharmaceutical field to increase drug solubility but has never been used before in the preparation of samples for DNP. With respect to the dissolution and melting approaches previously described, the mechanical milling offers several important advantages. First of all, it does not require the use of any solvent or glass forming agent which could decrease the polarization efficiency and/or introduce toxicologic issues. Second, a heating step is not required, thus preventing possible related problems as degradation or alteration of the radical or of the sub-

strate itself. Finally, the amorphous structure can be obtained through reproducible procedures thus allowing analysis and monitoring of the sample amorphization, or in other words allowing a quality control of the sample before hyperpolarization. For this reason mixtures obtained with the mechanical milling approach are really ready to use formulations, which can be used in the DNP process without the need of further critical preparation passages, and are hence especially valuable for the industrial applications.

The mechanical milling was shown to be an efficient approach for the amorphization of homogeneous mixtures of sugars, as trehalose, and radicals, as TEMPO [10]. Trehalose is a well-known non-reducing disaccharide of glucose widespread in most organisms, except vertebrates, which accumulates only in a few species, known as anhydrobionts. Relevance of trehalose in the biological word relies on its bioprotective properties [11]. In fact its synthesis is switched-on in cells exposed to stress conditions, giving the anhydrobiotic organisms the ability to be dehydrated, kept in a dormant state for long periods and rehydrated again to the original state [12]. In order to further improve the understanding of trehalose metamorphism, extensive studies have been carried out in solution and in solid state and, in particular, for its polymorphic transformations and amorphization [13–19]. Moreover, trehalose can be considered as a reference for the behaviour of non-ionic molecules undergoing fast dissolution in water and is able to form glass solutions with several other molecular materials by co-milling [20], paving the way for the preparation of multi-substrate DNP ready samples. The mechanical milling approach can be applied to any organic crystalline molecule stabilized by weak chemical bonds, such as Van der Waals, polar and/or H-bond interactions; more specifically the substrates are foreseen to belong to the group consisting of amino acids, carbohydrates, hydroxy-acids, dicarboxylic acids and ketoacids. All these biologically relevant compounds can in principle form either glassy formulations alone or in combination with others, such as trehalose. The DNP of  $^1\text{H}$  nuclei in trehalose was reported to reach a steady state nuclear polarization of 10% for TEMPO concentration around 0.5%, at a temperature  $T = 1.75$  K and in a magnetic field  $H = 3.46$  Tesla.

In the following we present an extensive study of the polarization efficiency of amorphous trehalose doped with TEMPO radicals by means of mechanical milling. The polarization rate and steady state polarization have been measured between 1.6 and 4.2 K for radical concentrations between 0.34% and 0.81%. Moreover, the temperature dependence of the nuclear spin-lattice relaxation rate  $1/T_1$  has been measured in order to obtain information on the microscopic mechanisms underlying the polarization process, an aspect which is relevant for the improvement of the final polarization level involved in the *in vivo* experiments. The results are fully consistent with a Thermal Mixing (TM) regime with a good contact between electron and nuclear spins.

## II. EXPERIMENTAL METHODS AND TECHNICAL ASPECTS

The samples of amorphous trehalose, doped with TEMPO radicals, were prepared according to the procedures reported in [10]. The final concentration of radicals obtained in the four investigated samples were expressed as the percentage of TEMPO mass with respect to the total sample mass: 0.34, 0.50, 0.64 and 0.81%. Accordingly, the samples will be hereafter indicated as T034, T050, T064, T081. The samples were the same ones previously used for the measurements reported in Ref. 10 except for T050, belonging to a later additional batch.

After preparation, all the samples were stored in fridge protected from light until the NMR measurement were performed, for a maximum time of 4 weeks. For all samples the cooling procedures consisted in a flash freezing, namely the sample holders were mounted on the DNP-NMR probe and immersed suddenly in liquid helium, without pre-freezing in liquid  $\text{N}_2$ , in approximately one minute.

The home-made DNP-NMR probe was inserted in a bath cryostat and placed inside the bore of a 3.46 Tesla superconducting magnet. The temperature inside the bath cryostat was controlled through helium adiabatic pumping between 1.6 K and 4.2 K. In order to perform DNP, all the samples were irradiated with a microwave (MW) source operating in the 96-98 GHz frequency range, with a nominal output power of 30 mW. The NMR signals were acquired with a solid-state Apollo Tecmag NMR spectrometer coupled to a  $^1\text{H}$  radiofrequency (RF) homemade probe tuned at 137.2 MHz.

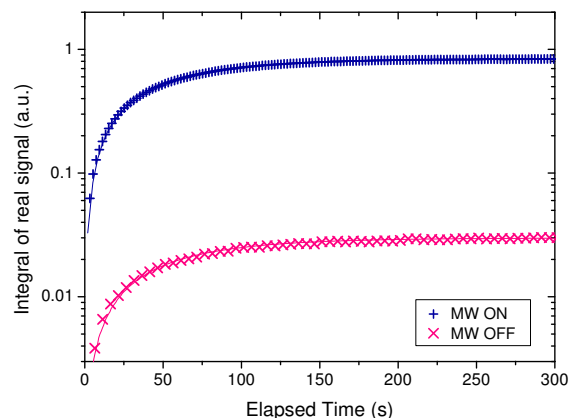


FIG. 1:  $^1\text{H}$  polarization build-up under MW irradiation (blue crosses) and without MW irradiation (pink crosses) in T034 at 4.2 K and 3.46 T. The solid lines are fits according to the buildup functions explained in the text (see Eq. 1).

For DNP experiments, the  $^1\text{H}$  polarization build-up

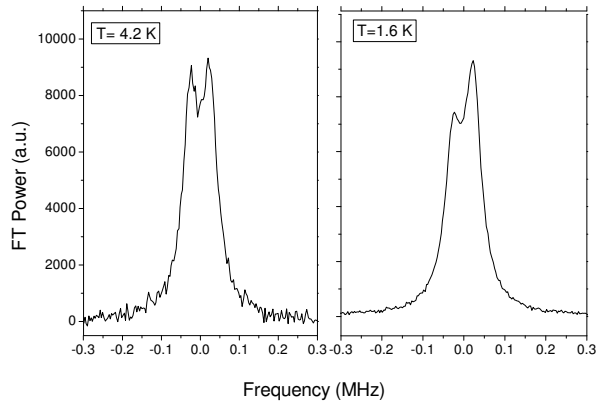


FIG. 2:  $^1\text{H}$  spectra in T050 obtained as the Fourier transform of the  $^1\text{H}$  free induction decay for steady-state polarization values under MW irradiation. The spectrum on the left has been measured at 4.2 K, while the spectrum on the right at 1.6 K.

(Fig. 1) was monitored under irradiation at the MW frequency maximizing the positive polarization enhancement. This frequency was set at about 97 GHz at 3.46 Tesla according to preliminary measurements carried out on a 3M reference Sodium Acetate solution in  $\text{D}_2\text{O}/\text{CD}_3\text{CD}_2\text{OD}(2/1)$  containing TEMPO 30 mM. After saturation with RF pulses, the  $^1\text{H}$  NMR signal was acquired up to steady state in the form of a Free Induction Decay (FID), by simply applying a series of low flip angle ( $6^\circ$ ) readout pulses [1], with a repetition time  $\tau$  of 2-5 s.

The polarization time constant  $T_{\text{pol}}$  was derived by fitting the build up curves to [21]

$$\frac{S(n\tau)}{S_\infty} = \left( 1 - \sum_{i=1}^n \cos \alpha^{i-1} (1 - \cos \alpha) \exp\left(-\frac{i\tau}{T_{\text{pol}}}\right) \right) - \exp\left(-\frac{n\tau}{T_{\text{pol}}}\right) \cos \alpha^n \quad (1)$$

which takes into account the reduction of the  $^1\text{H}$  signal amplitude induced by the readout pulses. Here  $S_\infty$  is the steady state  $^1\text{H}$  signal amplitude. In the absence of MW irradiation the same low flip angle sequence was used to measure the  $^1\text{H}$  build-up signal to the thermal equilibrium value after RF saturation (Fig. 1 - pink). Accordingly, Eq. (1) was used to retrieve the value of  $^1\text{H}$  spin-lattice relaxation time  $T_1$ .

The  $^1\text{H}$  polarization enhancement  $\epsilon$  reached values between 30 and 50 (Fig. 1) and was estimated by means of the following expression

$$\epsilon = \frac{S_{\infty\text{ON}}}{S_{\infty\text{OFF}}} \frac{RG_{\text{OFF}}}{RG_{\text{ON}}}, \quad (2)$$

where subscripts ON and OFF indicate that the microwaves are switched respectively ON and OFF. RG is

the receiver gain of the spectrometer which has been previously calibrated to confirm the linearity. Then, the nuclear polarization under MW irradiation  $P\%$  was calculated by multiplying the enhancement by the polarization thermal value, according to  $P\% = \epsilon \tanh(\gamma_H \hbar H / 2k_B T)$ , with  $\gamma_H$  the proton gyromagnetic ratio.

$^1\text{H}$  NMR spectra were obtained by means of the Fourier transform of the free induction decay (FID) signal. In all the investigated samples the spectra show the features visible in Figure 2. In absence of MW irradiation, the curve is characterized by two peaks of equal intensity and symmetrically shifted by  $\Delta = \pm 22$  kHz, while a clear asymmetry arises by irradiating with MW.

### III. EXPERIMENTAL RESULTS

The  $T$  dependence of the  $^1\text{H}$  Spin Lattice Relaxation (SLR) rates  $1/T_1$  and polarization rates  $1/T_{\text{pol}}$ , derived as explained in Section 2, are shown in Fig. 3 and 4, respectively. All the datasets indicate a fast increase of the rates with  $T$  between 1.6 and 4.2 K, which can be fit to a power law  $y(T) = AT^B$ , yielding the results reported in Table 1. From Table 1 and Figure 5 one can notice that the exponent  $B$  of the power law increases at low TEMPO concentration and saturates at about 2.7 above 0.5 %. Differently, the exponent  $B$  extracted from the fits of  $1/T_{\text{pol}}$  has a value close to 1.5, independent from the TEMPO concentration.

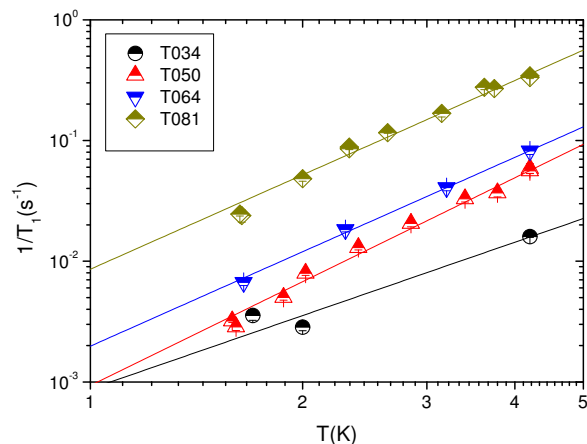


FIG. 3: Log-log plot of  $1/T_1(T)$  in all the investigated trehalose samples below 4.2 K. The solid lines are fits to the power law  $y(T) = AT^B$ , yielding the values reported in Table 1.

When reported as a function of the TEMPO concentration, at  $T = 2$  and 4.2 K (Fig. 6), both  $1/T_1$  and  $1/T_{\text{pol}}$  show a marked increase and can be fit again to power laws ( $y = ac^b$ ), retrieving the results summarized in Table 2, with  $b$  exponents taking values close to 3. It

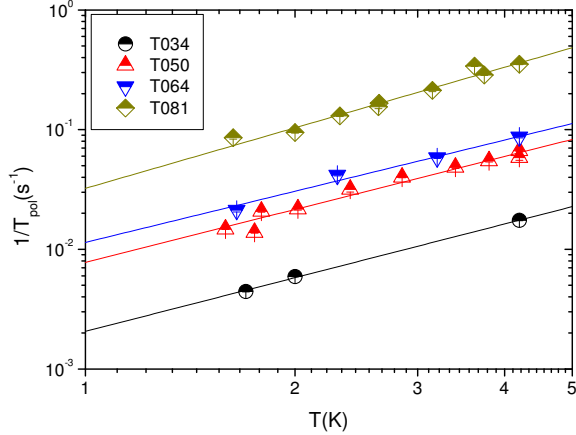


FIG. 4: Log-log plot of  $1/T_{\text{pol}}(T)$  in all the investigated trehalose samples below 4.2 K. The solid lines are fits to the power law  $y(T) = AT^B$ , yielding the values reported in Table 1.

TABLE I: Fit results of  $1/T_1(T)$  and  $1/T_{\text{pol}}(T)$ , at 3.46 Tesla, according to the law  $y(T) = AT^B$  in trehalose samples doped with TEMPO.

Sample	Measurement	A ( $\text{s}^{-1} \cdot \text{K}^{-B}$ )	B
T034	$1/T_1(T)$	$8.74 \pm 4.42 \times 10^{-4}$	$2.02 \pm 0.40$
T050	$1/T_1(T)$	$9.33 \pm 1.40 \times 10^{-4}$	$2.86 \pm 0.12$
T064	$1/T_1(T)$	$1.98 \pm 0.19 \times 10^{-3}$	$2.60 \pm 0.07$
T081	$1/T_1(T)$	$8.57 \pm 1.19 \times 10^{-3}$	$2.60 \pm 0.11$
T034	$1/T_{\text{pol}}(T)$	$2.06 \pm 0.09 \times 10^{-3}$	$1.49 \pm 0.04$
T050	$1/T_{\text{pol}}(T)$	$7.78 \pm 0.87 \times 10^{-3}$	$1.47 \pm 0.09$
T064	$1/T_{\text{pol}}(T)$	$1.14 \pm 0.17 \times 10^{-2}$	$1.42 \pm 0.13$
T081	$1/T_{\text{pol}}(T)$	$3.23 \pm 0.44 \times 10^{-2}$	$1.68 \pm 0.11$

is interesting to notice that at 4.2 K  $1/T_1$  and  $1/T_{\text{pol}}$  values are quite close for all samples, as observed in other DNP substrates [22]. On the other hand, around 2 K  $1/T_{\text{pol}} \sim 2/T_1$  in all samples.

TABLE II: Fit results of  $1/T_1(T)$  and  $1/T_{\text{pol}}(T)$  measurements according to the law  $y(T) = ac^b$  in trehalose samples, at  $T = 4.2$  K and 2 K, as a function of the ratio between the TEMPO weight and the sample weight.

T (K)	Measurement	a ( $\text{s}^{-1} \cdot \text{c}^{-b}$ )	b
4.2	$1/T_1(T)$	$0.67 \pm 0.15$	$3.37 \pm 0.30$
2	$1/T_1(T)$	$5.76 \pm 2.78 \times 10^{-2}$	$2.94 \pm 0.79$
4.2	$1/T_{\text{pol}}(T)$	$0.64 \pm 0.15$	$3.37 \pm 0.30$
2	$1/T_{\text{pol}}(T)$	$0.13 \pm 0.03$	$2.84 \pm 0.28$

Moreover, in all the investigated samples, the steady state  $^1\text{H}$  polarization P% grows on cooling. The highest P% of about 15% is obtained at 1.6 K for TEMPO concentrations of the order of 0.5%. These values are nearly

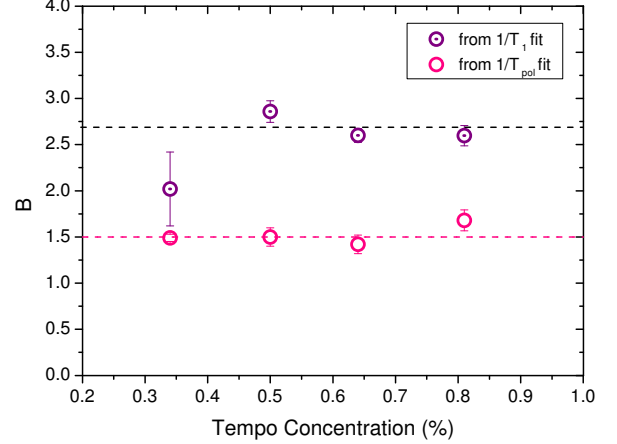


FIG. 5: The coefficient  $B$  obtained by the fits of  $1/T_1(T)$  (purple dotted circles) and of  $1/T_{\text{pol}}(T)$  (pink circles) reported as a function of the TEMPO concentration. The pink dotted curve corresponds to  $B = 1.5$ , the purple dotted line to  $B = 2.75$ .

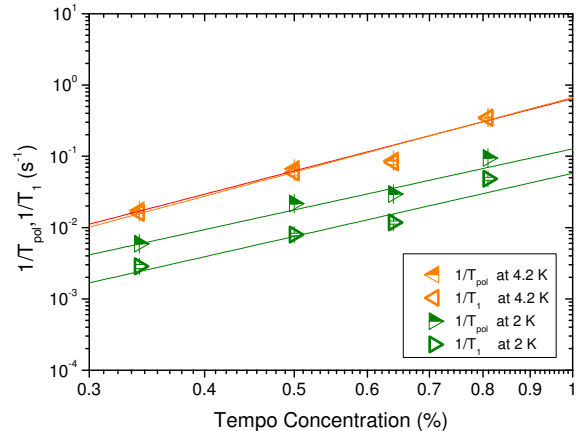


FIG. 6: Log-log plot of  $1/T_1(T)$  and  $1/T_{\text{pol}}(T)$  as a function of the TEMPO concentration in milled trehalose at 4.2 K and at 2 K. All the solid lines are fits to the power law  $y(T) = aT^b$  with parameters reported in Table 2.

twice the ones obtained at 0.81% in all the explored T range. In T050 P% increased by nearly 27% with respect to the one reported in Ref. 10, for  $T \simeq 1.75$  K (see Fig. 9). This increment of polarization can be ascribed to the lower temperature and possibly to a minor presence of water in the newly prepared sample. As shown in Fig. 7 for samples T050 and T081, P% reported as a function of  $1/T$  can be fit to a power law with a coefficient of the order of 1.6-1.8. The increase of P% correspondingly affects the shape of  $^1\text{H}$  spectra under MW irradiation obtained at low T. As depicted in Fig. 2 at 1.6 K the high



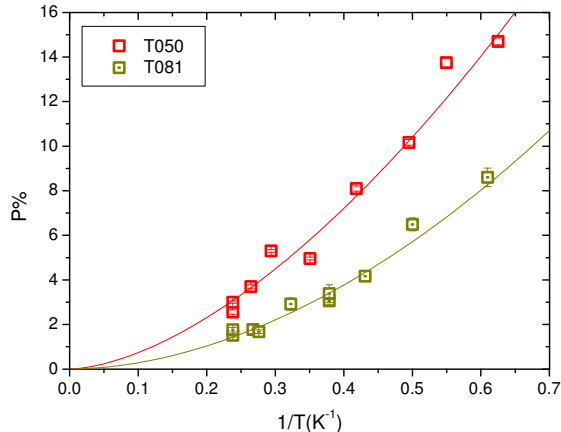


FIG. 7: P% as a function of  $1/T$  in T050 (red squares) and T081 (green dotted squares). The solid lines are fits to the power law  $y(T) = aT^b$ , yielding  $b = -1.64 \pm 0.12$  for T050 (red curve) and  $b = -1.86 \pm 0.12$  for T081 (blue curve)

frequency peak grows in intensity at the expenses of the low frequency peak. In principle, this structure could be interpreted resorting to a dipolar Pake Doublet model for close pairs of protons (e.g. protons of  $\text{CH}_2$ ) and, consistently, in this framework the growth of the high frequency peak would reflect the increase of the number of spin-up protons due to MW irradiation [23]

It is noticed that the relaxations times in amorphous trehalose doped with TEMPO are shorter than 1100 s for  $T \rightarrow 1$  K (Fig. 3) while in frozen solutions of NaOAc and glycine with 30mM TEMPO they range between 2000 and 7500 s [7]. For glycine in water/glycerol the maximum polarization (29.4 %) is obtained with 45 mM TEMPO, and at 1.2 K the polarization and relaxation times are 460 and 4800 s, respectively. In the trehalose sample showing the maximum polarization (T050) one can estimate significantly shorter time scales, a polarization time of 125 s and a relaxation time of 1000 s. In spite of this substantial difference, the maximum polarization of 15% reached in T050 at 1.6 K is just modestly lower than the one obtained in the frozen solutions. In fact, on considering the simplified high temperature relation for the polarization  $P \simeq B/T$  invoked by Kurdzseau et al, [7], one finds that at 1.6 K the polarization of glycine in water/glycerol with 45 Mm TEMPO rescales to 21% and the one of NaOAc in water/ethanol with 30 mM TEMPO to 17.8%, quite close to the one reached in T050. Hence, in different samples containing the same amount of radical, the polarization rates depend significantly on the dynamic properties of the substrate. The short relaxation times observed in trehalose samples are likely due to a significant reduction of the electronic relaxations times in these samples with respect to frozen solutions. For reference, one could consider that  $T_{1e} \simeq 310\text{ms}$  for a concentration 5 mM of TEMPO in a solution with wa-

ter/glycerol, at 1.55 K and 3.35 Tesla [24].

## IV. DISCUSSION

### A. Nuclear spin-lattice relaxation

We shall start discussing the different contributions to the nuclear SLR rates. In the investigated systems  $^1\text{H}$  SLR can be expressed in principle as the sum of independent terms:

$$\frac{1}{T_1} = \left(\frac{1}{T_1}\right)_{1H-1H} + \left(\frac{1}{T_1}\right)_{el}, \quad (3)$$

where  $(1/T_1)_{1H-1H}$  sums up the contributions from intra and intermolecular proton-proton dipolar interactions and  $(1/T_1)_{el}$  is the contribution due to the hyperfine coupling with the radical electron spins <sup>1</sup>. The term due to the hyperfine interactions with the electrons is reasonably the dominant one, as suggested by the dependence of  $1/T_1$  on the radical concentration  $c$ . If a sizeable relaxation not involving the electron spins was present, one should fit the data in Fig. 6 with a sum of a power law and a non negligible constant term  $y(c) = ac^b + \text{const}$ . In order to estimate that constant term one can notice that in a sample of milled pure trehalose at 0.87 Tesla and 4.2 K  $^1\text{H}$   $1/T_1(T) \simeq 0.01\text{s}^{-1}$ . Now, if one considers that at low temperature a slow motion regime is attained yielding a frequency dependence  $1/T_1 \sim 1/\omega_H^2$  ( $\omega_H$   $^1\text{H}$  Larmor frequency), one estimates  $1/T_1 \simeq 6 \times 10^{-4}\text{s}^{-1}$  at 3.46 Tesla, more than two orders of magnitude smaller than the experimental values.

Accordingly, one has that  $1/T_1 \simeq (1/T_1)_{el}$ . The SLR due to the interaction with the electrons can in turn be described as the sum of two terms

$$\frac{1}{T_1} = \left(\frac{1}{T_1}\right)_{el} \simeq \left(\frac{1}{T_1}\right)_l + \left(\frac{1}{T_1}\right)_p, \quad (4)$$

where  $(1/T_1)_l$  is the relaxation driven by the amorphous lattice dynamics and  $(1/T_1)_p$  is the relaxation through the electron spin-lattice relaxation channel, in particular through ISS processes (where I are nuclear spins and S electron spins) to be explained in Sec. 4.2, which are particularly efficient in these samples thanks to a good thermal contact between electron and nuclear spin reservoirs.

At low temperature,  $T < 4.2$  K, the first contribution is associated with a modulation of the nuclear-electron couplings by the low frequency glassy dynamics. The same process was observed also in pyruvic acid organic

<sup>1</sup> Here we neglect the contribution due to heteronuclear interactions with  $^{13}\text{C}$  and  $^{17}\text{O}$  isotopes of trehalose molecules which have very low natural abundance and with other spin active nuclei of the TEMPO molecule, contained in mM concentration.

glass doped with trityls [22]. As explained in that framework, glasses can be characterized by a distribution of local lattice dynamics which control the behaviour of several physical properties. In particular upon increasing  $T$  each molecule or atom can fluctuate among different energy minima separated by a barrier  $\Delta E$ , on a time scale described by a correlation time  $\tau_c(T) = \tau_0 \exp(\Delta E/T)$ , with  $\tau_0$  the correlation time at  $T \gg \Delta E$ .

For each activation barrier,  $1/T_1$  can be described by resorting to a spectral density of the form [25]

$$\left(\frac{1}{T_1}\right)_l = \frac{\gamma_H^2 \langle \Delta h_\perp^2 \rangle}{2} J(\omega_L) = \frac{\gamma_H^2 \langle \Delta h_\perp^2 \rangle}{2} \frac{2\tau_c}{1 + \omega_L^2 \tau_c^2}, \quad (5)$$

where  $\langle \Delta h_\perp^2 \rangle$  is the mean square amplitude of the random fluctuating fields probed by the nuclei in the plane perpendicular to  $\vec{H}$ . By considering different types of distribution functions  $p(\Delta E)$ , a low- $T$  power-law behaviour with  $1/T_1 \sim T^{1+\alpha}$  ( $0 \leq \alpha \leq 1$ ) is found [26, 27]. In particular in pyruvic acid a quadratic power law  $1/T_1 \sim T^2$  was observed for the relaxation due to glassy modes [22], which can be obtained for  $p(\Delta E) \propto \Delta E$ .

Eq. 5 can be further specialized by assuming that the lattice modes are characterized by low-frequency fluctuations yielding  $\omega_H \tau_c \gg 1$ . This is suggested by the observation that at 4.2 K in an equivalent preparation of amorphous Lactose  $1/T_1 \propto 1/\omega_H^2$ , a dependence typical of the slow motion limit. In such conditions Eq.5 reduces to  $1/T_1(T) \propto \gamma_H^2 \langle \Delta h_\perp^2 \rangle \langle 1/\tau_c(T) \rangle$ , where  $\langle 1/\tau_c \rangle$  represents an average correlation frequency of the fluctuations over the distribution  $p(\Delta E)$ . Now, by expressing  $\langle \Delta h_\perp^2 \rangle$  in Eq. 5 in terms of the dipolar interaction with the electrons, it is possible to write[25]

$$\left(\frac{1}{T_1}\right)_l = \frac{2}{5} \left(\frac{\mu_0}{4\pi}\right)^2 \frac{\gamma_e^2 \gamma_e^2 \hbar^2 S(S+1)}{\omega_H^2} \left\langle \frac{1}{r_{eH}^6} \right\rangle \left\langle \frac{1}{\tau_c} \right\rangle, \quad (6)$$

where  $S$  is the electron spin,  $\gamma_e$  the electron gyromagnetic ratio and  $r_{eH}$  the electron-proton distance. Such contribution to  $1/T_1$  is seemingly more important in samples with low radical concentration, where the less efficient thermal contact between electron and nuclear spins lowers  $(1/T_1)_p$ . In fact, in T034, the sample having the lowest polarization, one finds  $1/T_1 \sim T^2$ , as observed in pyruvic acid for the relaxation rates of protons driven by the glassy dynamics [22].

Thus, even if a contribution of  $(1/T_1)_p$  is expected also for T034, one can estimate an upper limit for  $\langle 1/\tau_c(T) \rangle$  by assuming that  $1/T_1(T)$  of T034 is originating only from the modulation of the dipolar interaction by the glassy dynamics. In this sample, from the average distance among radicals, one can estimate [22] the root mean square amplitude  $\sqrt{\langle \Delta h_\perp^2 \rangle} = 26.44 \times 10^{-4}$  Tesla at the  $^1\text{H}$  site and  $\langle 1/\tau_c(T) \rangle \simeq AT^B$  with  $A = 3.74 \times 10^3 \text{ s}^{-1} \cdot \text{K}^{-B}$  and  $B = 2.02$ , values very close to the ones describing the glassy dynamics in pyruvic acid [22]. Since Eq. 6 gives a linear dependence of  $(1/T_1)_l$  on the radical concentration, by considering this average correlation

frequency, one would derive  $(1/T_1)_l = 1.28 \times 10^{-3} T^2$  in T050,  $(1/T_1)_l = 1.64 \times 10^{-3} T^2$  in T064 and  $(1/T_1)_l = 2.08 \times 10^{-3} T^2$  in T081. These values are lower than the experimental relaxation rates in all samples with concentration larger than 0.34%. The relaxation rates have a more pronounced  $T$  dependence, close to  $1/T_1 \sim T^{2.75}$ , on the other hand, the rates increase according to  $1/T_1 \sim c^3$ , as  $1/T_{\text{pol}}$ . This confirms, as it will be shown in the next Section, that the contribution to the SLR due to the glassy dynamics can be neglected and confirms that the relaxation and polarization rates must originate from the same process involving the thermal contact between nuclear and electron spins.

## B. Dynamic nuclear polarization

We will now discuss the nature of the polarization regime attained in amorphous trehalose doped with TEMPO on the basis of the experimental data. In particular, in close analogy with the considerations of Kurdzseau et al. [7] about the behaviour of frozen solution with TEMPO, the presence of Thermal Mixing is likely also in trehalose samples [1, 6, 8]. In a range of radical concentrations between 30-80 mM the electrons are strongly coupled by the dipolar interaction and a relevant communication of the spin temperature among spin packets across the electron resonance line can develop. Moreover, in presence of TEMPO radicals, the  $\omega_H$  of protons is smaller than the electron spin resonance (ESR) linewidth, thus the nuclear and the electron spins can directly interact by means of a three body interaction, dipolar in nature. Throughout this mechanism indicated briefly as ISS, transitions at  $\hbar\omega_H$  flipping one nuclear spin  $I$  can be promoted by the flip-flop excitations of couples of electron spins ( $S$ ). As a result, nearly the whole reservoir of  $N_n$  nuclei can get in contact with the whole reservoir of  $N_e$  electrons in dipolar interaction and hence realize the Thermal Mixing, which tends to equalize their spin temperatures.

In particular, when the electron-nucleus ISS contact is very efficient  $T_{\text{ISS}}/T_{1e} \ll 1$ , with  $T_{\text{ISS}}$  the contact time between nuclei and electrons, the electron relaxation processes act as a bottle neck for the nuclear relaxation and polarization processes [22, 28–30]. Therefore for the relaxation rates induced by the Thermal Mixing and the polarization rates one finds [22]

$$(1/T_1(T))_{el} = 1/T_{1e}(T)(N_e/N_n)[1 - P_0(T)^2], \quad (7)$$

and

$$(1/T_{\text{pol}}(T)) = 1/T_{1e}(T)(N_e/N_n), \quad (8)$$

where  $N_e/N_n$  is the ratio between the radical and the nuclei concentration and  $P_0(T)$  is the electron thermal polarization. The two equations above give a clear pictorial view of the physical process underlying and connecting

relaxation and polarization: the ISS mechanism originating TM is able to flip one of the  $N_n$  nuclear spins, as long as one of the  $N_e$  electrons relaxes to thermal equilibrium in the time  $T_{1e}$ . The factor  $[1 - P_0(T)^2]$  is the only one differentiating the relaxation rates from the polarization rates and, in absence of MW irradiation, it represents the reduction of the flip-flops probability due to the gradual filling of the lowest electron spin level at low temperatures.

The fact that both  $1/T_1$  and  $1/T_{pol}$  scale as  $c^3$  (see previous Section) further supports the presence of a good thermal contact and indicates, according to Eqs. 7 and 8, that  $1/T_{1e} \sim c^2$ . This power-law can be justified by considering that  $1/T_{1e} \propto \langle \Delta_e^2 \rangle$ , the square of the field distribution probed by electron spins in dipolar interaction, which at very low concentrations ( $N_e/N_n \ll 1$ ) scales as  $c^2$ . [25, 31]

In order to discuss the DNP mechanisms in amorphous trehalose samples we shall now analyze the relation between polarization and relaxation rates obtained at different T for various radical concentrations. In particular, by reporting for each sample the experimental  $y = 1/T_1$  values as a function of  $x = (1/T_{pol}) [1 - P_0(T)^2]$ , one notices that the values approach the linear  $y = x$  relation, according to Eqs. 7 and 8, for TEMPO concentrations of 0.5%, while the relation approaches  $y = 1.28x$  on increasing the TEMPO concentration to 0.8%. The sample T050 is correspondingly the one showing the highest polarization values both as a function of T and as a function of radical concentration. In fact according to previous results, the nuclear polarization in these systems displays a peak for TEMPO concentrations of 0.5% which correspond to radicals molar concentration around 50 mM (Fig. 9 [10]).

These observations closely recall the ones explained in previous papers reporting the polarization properties of frozen glassy solutions of NaOAc and glycine, dissolved in water/ethanol and water/glycerol and containing TEMPO radicals, around 1.2 K [7]. Remarkably, on expressing the  $y = 1/T_1$  values as a function of  $x = (1/T_{pol}) [1 - P_0(T)^2]$  reported in Table I and II of Kurdzesau et al. [7] for protons, one finds  $y = x$ , as in T050. Moreover, the nuclear polarization as a function of TEMPO concentration follows a non monotonic behaviour, as it is observed here, with a maximum value approached at a lower TEMPO concentration, around 30 mM.

Definitely, in all trehalose samples the TM is likely attained but other relaxation mechanisms arise when the electron concentration is varied. On one hand, since a fit of the experimental data with the law  $y = \alpha x$  holds, one definitely concludes that the SLR rate due to the glassy dynamics is negligible. If that contribution was present, a non-zero intercept on the y-axis should have been observed. On the other hand  $\alpha$  different from 1 in samples with concentrations lower or higher than 0.5% could reflect different scenarios. In T034, where  $\alpha = 1.24$  the polarization is less pronounced with respect to the

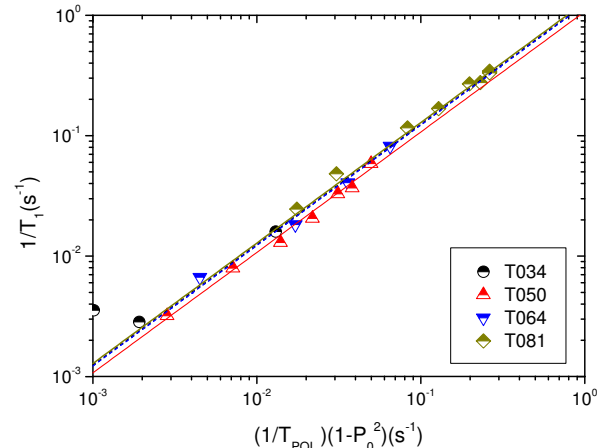


FIG. 8:  $1/T_1$  in all the investigated trehalose samples reported as a function of  $1/T_{pol}(1 - P_0^2)$  measured in the same sample and around the same temperature. The lines represent the fits to the power law  $y(T) = \alpha x$ , yielding the values  $\alpha = 1.24 \pm 0.12$  for **T034**,  $\alpha = 1.07 \pm 0.04$  for T050,  $\alpha = 1.22 \pm 0.04$  for T064 and  $\alpha = 1.28 \pm 0.02$  for T081. The red solid line represents the fit of T050 data, the closest ones to  $y = x$ , while the green solid line represents the fit of T081 data, the farther ones from  $y = x$ .

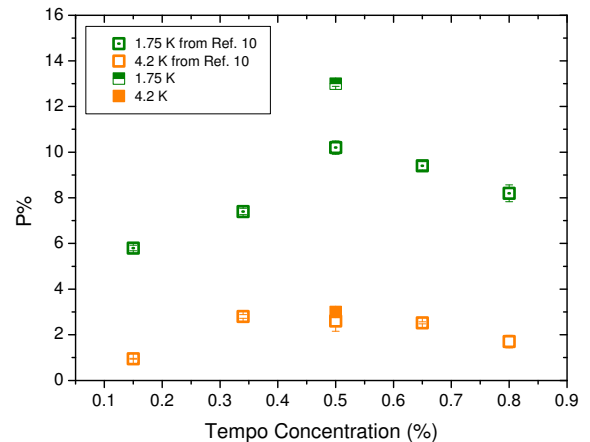


FIG. 9: P% as a function of radical concentration in all the investigated trehalose samples at 1.75 K (green dotted squared) and 4.2 K (orange squares). The filled squares represent the data collected in the new T050 considered in this work.

other samples. This could arise from a degradation of the electron-nucleus contact induced by the increased average electron-nucleus distances. Moreover, the electron-electron dipolar couplings, which enable rapid spectral spin diffusion within the broad inhomogeneous ESR line of TEMPO, get weaker in this sample and a smaller frac-

tion of the electron spins can contribute to the DNP process.

For high TEMPO concentrations of 0.81 %  $\alpha$  deviates from 1, increasing to 1.28 in T081. Nevertheless, the presence of a good contact between nuclei and electrons, evidenced by the high relaxation and polarization rates, indicates that the nuclear relaxation originating from the contact with the electron reservoir should be considered as enhanced with respect to the optimal good contact case. One possible explanation for this enhancement of the linear coefficient is that, on increasing the electron concentration, the thermal contact between electrons and protons occurs via additional processes with respect to ISS, so that the factor  $1 - P_0(T)^2$  is modified. A detailed explanation of these terms requires a microscopic description [32].

Definitely, the order of magnitude of polarization, relaxation and polarization times in these materials are consistent with the TM regime, however the experimental  $P\%$  (Fig. 7) as a function of  $1/T$  clearly displays a non linear trend at low  $T$  (i.e. on increasing  $1/T$ ) which cannot be explained in the framework of the traditional Borghini model of TM. As in pyruvic acid doped with trityls [22], this non linear behaviour can still be explained within the TM by considering dissipation mechanism affecting directly the electron reservoir only, such as limited microwave power [29, 33] or the dissipative processes in the spectral diffusion [30].

## V. CONCLUSIONS

An extensive study of amorphous samples of trehalose sugar doped with TEMPO radicals by means of mechanical milling has evidenced that in the 1.6-4.2 K range the relaxation and polarization properties sensibly depend on temperature and radical concentration. Upon spanning the concentration range  $0.34 \div 0.81\%$  the samples displayed a non monotonic behaviour of the steady-state nuclear polarization with a peak of 15% around 0.5 %. The temperature and concentration dependence of the spin lattice relaxation and polarization rates in

all samples followed power laws with coefficients close to 2.7 and 3, respectively. These coefficients are compatible with the hypothesis of a dominant coupling between nuclei and electrons driving both nuclear spin-lattice relaxation and DNP. Differently from other glassy systems, in trehalose the glassy dynamics causes a negligible contribution to the relaxation. The proportionality  $1/T_1 = 1/T_{pol} [1 - P_0(T)^2]$  in the investigated samples is consistent with the presence of TM and a good contact between the nuclei and the electrons. However, on increasing electron concentration, some additional relaxation channels, also responsible for the decrease of the nuclear polarization, must be considered. Definitely the aforementioned results evidence very good polarization performances of trehalose sugar doped with TEMPO radicals by means of mechanical milling. While the polarization levels are just slightly lower than the ones obtained in the standard frozen solutions, one observes significantly shorter relaxation and polarization times. These results provide further support in favour of the applicability of sugars mixed with TEMPO by mechanical milling for the DNP and for their application for *in vivo* molecular imaging. In perspective the same preparation approach could be applied to other substrates as amino acids, carbohydrates, hydroxy-acids, dicarboxylic acids and ketoacids.

## Acknowledgements

This study has been supported in part by the COST Action TD1103 (European Network for Hyperpolarization Physics and Methodology in NMR and MRI) and by a public grant from the "Laboratoire d'Excellence Physics Atom Light Mater" (LabEx PALM) overseen by the French National Research Agency (ANR) as part of the "Investissements d'Avenir" program (reference: ANR-10-LABX-0039). E. Elisei has been supported by Bracco Imaging S.p.A. and by the PhD School on Nanotechnology of the University of Trieste.

- 
- [1] J. H. Ardenkjaer-Larsen, B. Fridlund, A. Gram, G. Hansson, L. Hansson, M. H. Lerche, R. Servin, M. Thaning, and K. Golman, *PNAS* **100**, 10158 (2003).
  - [2] P. Dutta, G. V. Martinez, and R. J. Gillies, *Biophys. Rev.* **5**, 271 (2013).
  - [3] A. B. Barnes, G. De Paepe, P. C. A. van der Wel, K.-N. Hu, C.-G. Joo, V. S. Bajaj, M. L. Mak-Jurkauskas, J. R. Sirigiri, J. Herzfeld, R. J. Temkin, et al., *Applied Magnetic Resonance* **34**, 237 (2008), ISSN 0937-9347, URL <http://dx.doi.org/10.1007/s00723-008-0129-1>.
  - [4] Q. Z. Ni, E. Daviso, T. V. Can, E. Markhasin, S. K. Jawla, T. M. Swager, R. J. Temkin, J. Herzfeld, and R. G. Griffin, *Accounts of Chemical Research* **46**, 1933 (2013), pMID: 23597038, <http://dx.doi.org/10.1021/ar300348n>, URL <http://dx.doi.org/10.1021/ar300348n>.
  - [5] A. J. Rossini, A. Zagdoun, M. Lelli, A. Lesage, C. Copret, and L. Emsley, *Accounts of Chemical Research* **46**, 1942 (2013), pMID: 23517009, <http://dx.doi.org/10.1021/ar300322x>, URL <http://dx.doi.org/10.1021/ar300322x>.
  - [6] A. Comment, B. van den Brandt, K. Uffmann, F. Kurdzesau, S. Jannin, J. Konter, P. Hautle, W. Wenckeback, R. Gruetter, and J. van der Klink, *Concepts in Magnetic Resonance Part B: Magnetic Resonance Engineering* **31B**, 255 (2007).
  - [7] F. Kurdzesau, B. van den Brandt, A. Comment,



- P. Hautle, S. Jannin, J. J. van der Klink, and J. A. Konter, *J. Phys. D: Appl. Phys.* **41**, 155506 (2008).
- [8] J. H. Ardenkjaer-Larsen, S. Macholl, and H. Johanneson, *Appl. Magn. Res.* **34**, 509 (2008).
- [9] T.-C. Ong, M. L. Mak-Jurkauskas, J. J. Walsh, V. K. Michaelis, B. Corzilius, A. A. Smith, A. M. Clausen, J. C. Cheetham, T. M. Swager, and R. G. Griffin, *The Journal of Physical Chemistry B* **117**, 3040 (2013), PMID: 23421391, <http://dx.doi.org/10.1021/jp311237d>, URL <http://dx.doi.org/10.1021/jp311237d>.
- [10] E. Elisei, M. Filibian, P. Carretta, S. Colombo Serra, F. Tedoldi, J. F. Willart, M. Descamps, and A. Cesàro, *Chem. Commun.* **51**, 2080 (2015), URL <http://dx.doi.org/10.1039/C4CC08348B>.
- [11] J. H. Crowe, F. A. Hoekstra, and L. M. Crowe, *Ann. Rev. Physiol.* **54**, 579 599 (1992).
- [12] K. I. Jönsson and R. Bertolani, *J. Zool.* **255**, 121 (2001).
- [13] F. Sussich, R. Urbani, P. F., and A. Cesàro, *J. Am. Chem. Soc.* **120**, 7893 (1998).
- [14] J. F. Willart, A. De Gusseme, S. Hemon, G. Odou, F. Danede, and M. Descamps, *Solid State Communications* **119**, 501 (2001), ISSN 0038-1098, URL <http://www.sciencedirect.com/science/article/pii/S0038109801002836>, pp. 8416–8428 (2013).
- [15] O. S. McGarvey, V. L. Kett, and D. Q. Craig, *The Journal of Physical Chemistry B* **107**, 6614 (2003).
- [16] F. Sussich, S. Bortoluzzi, and A. Cesàro, *Thermochim. Acta* **391**, 137 (2002).
- [17] F. Sussich and A. Cesàro, *Carbohydrate Research* **343**, 2667 (2008).
- [18] H. Nagase, N. Ogawa, T. Endo, M. Shiro, H. Ueda, and M. Sakurai, *The Journal of Physical Chemistry B* **112**, 9105 (2008).
- [19] D. Kilburn and P. E. Sokol, *The Journal of Physical Chemistry B* **113**, 2201 (2009).
- [20] A. M. Gil, P. S. Belton, and V. Felix, *Spectrochimica Acta Part A: Molecular and Biomolecular Spectroscopy* **52**, 1649 (1996).
- [21] G. Pages and P. W. Kuchel, *Magnetic Resonance Insights* **6** (2013).
- [22] M. Filibian, S. Colombo Serra, M. Moscardini, A. Rosso, F. Tedoldi, and P. Carretta, *Phys. Chem. Chem. Phys.* **16**, 27025 (2014), URL <http://dx.doi.org/10.1039/C4CP02636E>.
- [23] these properties will be analyzed and discussed in another paper (????).
- [24] J. Granwehr, J. Leggett, and W. Kockenberger, *Journal of Magnetic Resonance* **187** (2007).
- [25] A. Abragam, *Principles of Nuclear Magnetism* (Oxford University Press, 1983).
- [26] S. Estalji, O. Kanert, J. Steinert, H. Jain, and K. Ngai, *Phys. Rev. B* **43**, 7481 (1991).
- [27] S. K. Misra, *Spectrochimica Acta Part A* **54**, 2257 (1998).
- [28] S. Colombo Serra, A. Rosso, and F. Tedoldi, *Phys. Chem. Chem. Phys.* **14**, 13299 (2012).
- [29] S. Colombo Serra, A. Rosso, and F. Tedoldi, *Phys. Chem. Chem. Phys.* **15**, 1002836 (2013), pp. 8416–8428 (2013).
- [30] S. Colombo Serra, M. Filibian, P. Carretta, A. Rosso, and F. Tedoldi, *Phys. Chem. Chem. Phys.* **16**, 753 (2014).
- [31] R. Berger, J. Kliava, E. M. Yahiaoui, J. C. Bissey, P. K. Zinsou, and P. Beziade, *Journal of non-crystalline solids* **180**, 151 (1995).
- [32] A. De Luca and A. Rosso, *Phys. Rev. Lett.* **115**, 080401 (2015), URL <http://link.aps.org/doi/10.1103/PhysRevLett.115.080401>.
- [33] S. Jannin, A. Comment, and J. J. van den Klink, *Appl. Magn. Res.* **43**, 59 (2012).